



## Original Article

## Efficiency calibration and coincidence summing correction for a NaI(Tl) spherical detector

Salam F. Nouredine<sup>a</sup>, Mahmoud I. Abbas<sup>b</sup>, Mohamed S. Badawi<sup>b, c, \*</sup><sup>a</sup> Physics Department, Faculty of Science, Lebanese University, Beirut, Lebanon<sup>b</sup> Physics Department, Faculty of Science, Alexandria University, Alexandria, Egypt<sup>c</sup> Department of Physics, Faculty of Science, Beirut Arab University, Beirut, Lebanon

## ARTICLE INFO

## Article history:

Received 16 July 2020

Received in revised form

8 April 2021

Accepted 13 April 2021

Available online 19 April 2021

## Keywords:

Spherical NaI(Tl) detector

Effective solid angle

Efficiency transfer method

Numerical analytical method

Coincidence summing factors

## ABSTRACT

Spherical NaI(Tl) detectors are used in gamma-ray spectrometry, where the gamma emissions come from the nuclei with energies in the range from a few keV up to 10 MeV. A spherical detector is aimed to give a good response to photons, which depends on their direction of travel concerning the detector center. Some distortions in the response of a gamma-ray detector with a different geometry can occur because of the non-uniform position of the source from the detector surface. The present work describes the calibration of a NaI(Tl) spherical detector using both an experimental technique and a numerical simulation method (NSM). The NSM is based on an efficiency transfer method (ETM, calculating the effective solid angle, the total efficiency, and the full-energy peak efficiency). Besides, there is a high probability for a source-to-detector distance less than 15 cm to have pulse coincidence summing (CS), which may occur when two successive photons of different energies from the same source are detected within a very short response time. Therefore,  $\gamma$ - $\gamma$  ray CS factors are calculated numerically for a  $^{152}\text{Eu}$  radioactive cylindrical source. The CS factors obtained are applied to correct the measured efficiency values for the radioactive volumetric source at different energies. The results show a good agreement between the NSM and the experimental values (after correction with the CS factors).

© 2021 Korean Nuclear Society, Published by Elsevier Korea LLC. This is an open access article under the CC BY-NC-ND license (<http://creativecommons.org/licenses/by-nc-nd/4.0/>).

## 1. Introduction

In some applications, a NaI(Tl) scintillation detector is used to determine the radioactivity of environmental samples and wastes. This is because of its relative simplicity of use, which doesn't need cooling of the crystal [1–8]. Such measurements normally require a close geometry arrangement with sources of different forms. The short distance between the source and the detector surface increases the probability of the coincidence summing (CS) phenomenon for a radionuclide with a complex decay scheme. The correction of these phenomena is not normally simple, especially for volumetric radioactive sources [9]. Consequently, for greater precision in gamma-ray spectrometry, corrections for the CS effect are extremely desirable [10–12].

By using the efficiency transfer method [9], the detector efficiency curve can be obtained for any measurement conditions, even

for those different from the calibration ones. The detector efficiency values can be obtained based on the change in the effective solid angle ratio, for any geometrical arrangement and quite a few samples at unusual distances from the detector surface [13–16]. In prior studies, NaI(Tl) detectors were used in different geometries in the form of a borehole, a parallelepiped with a rectangular hole, a cylinder, etc. This is due to the low cost of preparation of the crystal, its high mass number, high efficiency, and room-temperature operation. A spherical NaI(Tl) detector has a wide solid angle subtended between the source-to-detector system in comparison with other detectors such as well-type detectors [17–20].

In the current work, CS effects in gamma-ray spectrometry are examined for a spherical detector with a diameter  $2R_d = 7.6$  cm. The effective solid angles and the full-energy peak efficiency in the case of radioactive point and cylindrical sources are determined by a new numerical simulation method (NSM). Besides, the total efficiencies are calculated to determine the CS factors. The radioactive point sources are simulated at axial and non-axial positions from the spherical detector axis, where the axial axis is the vertical one and the non-axial position has a lateral displacement from the axial axis. This study is then extended and generalized to determine the

\* Corresponding author. Physics Department, Faculty of Science, Alexandria University, Alexandria, Egypt.

E-mail addresses: [ms241178@hotmail.com](mailto:ms241178@hotmail.com), [m.badawi@bau.edu.lb](mailto:m.badawi@bau.edu.lb) (M.S. Badawi).

efficiencies with radioactive cylindrical sources.

The efficiency transfer method is used as the core of the NSM. It is possible to determine the detector efficiency of the radioactive cylindrical source at different distances from the detector surface. The formulas have been solved with Mathcad 14 and programmed in the BASIC language. To show the strength of this new method, experimental measurements have been performed at the Radiation Physics Laboratory (Laboratory of Prof. Younis S. Selim), Faculty of Science, Alexandria University, Egypt. These measurements have been done with several standard radioactive sources of different energies, which were purchased from the Physikalisch-Technische Bundesanstalt (PTB), Germany. The sources have been placed on a Plexiglas holder at different distances from the surface of the detector. The results after the CS corrections in the case of the volumetric source show a good performance of the NSM.

The present article is organized as follows: Section 2 presents in detail the NSM, including the calculation of the effective solid angle, the total efficiency, and the full-energy peak efficiency considering different radioactive sources, which are positioned axially and non-axially concerning the spherical NaI(Tl) detector vertical axis. Section 3 describes the experiments. Section 4 contains a comparison of the values calculated by the NSM for the spherical NaI(Tl) detector with measurements, giving an idea of the applicability of the current approach. Conclusions are presented in Section 5.

### 2. Mathematical viewpoint

The total efficiency of a NaI(Tl) spherical detector,  $\epsilon_{T(Point)}$  for an axial radioactive point source can be calculated according to the following equation in the spherical coordinate form [21].

$$\epsilon_{T(Point)} = \frac{\Omega_{ref[Axial]}}{4\pi} \tag{1}$$

where  $\Omega_{ref[Axial]}$  is the effective solid angle subtended by an isotropically radiating point-like source situated axially at a distance  $h$  from the detector active medium surface (as shown in Fig. 1) and is given by

$$\Omega_{ref[Axial]} = \int_0^{2\pi} \int_0^{\theta_{max}} f_{att} (1 - e^{-\mu d}) \sin\theta \, d\theta d\phi \tag{2}$$

The polar angle,  $\theta$ , takes values between 0 and the maximum polar angle,  $\theta_{max}$  that allows photons to go through the detector. The angle  $\theta_{max}$  depends on the height,  $h$ , and the detector radius,  $R_d$ , as

$$\theta_{max} = \sin^{-1} \left( \frac{R_d}{\sqrt{(R_d+h)^2}} \right) \tag{3}$$

The distance,  $d$ , traveled by the photons through the active medium of the detector can be calculated by the following expression

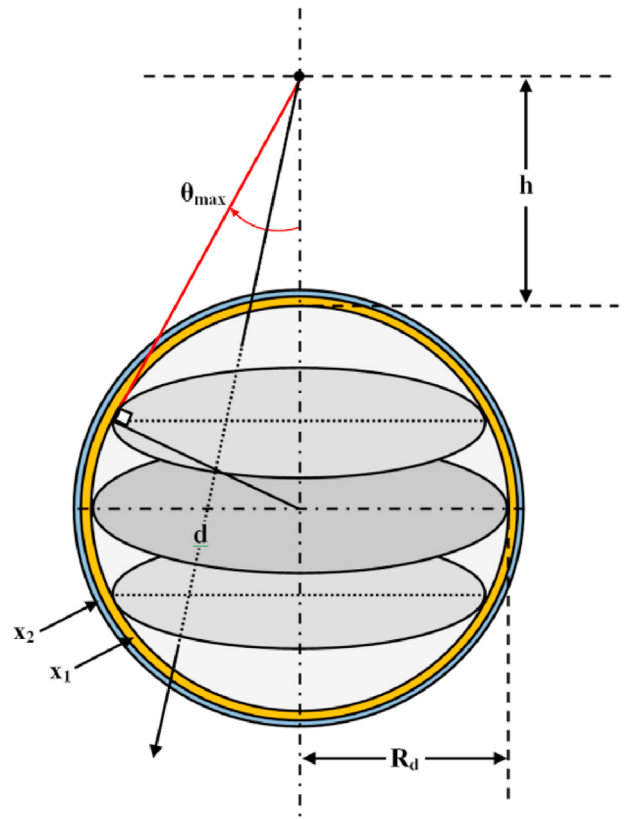


Fig. 1. Isotropically radiating point source situated at a distance,  $h$ , from the spherical detector surface.

$$d = 2 \sqrt{R_d^2 - [\rho^2 + (R_d+h)^2] \sin^2\theta} \tag{4}$$

where  $\rho$  is the lateral displacement if the point source is in a non-axial position.

The attenuation factor,  $f_{att}$ , is due to the reflector, the end cap, and the absorber between the source and the detector active medium. These parts are described as absorber layers with attenuation coefficients  $\mu_1, \mu_2, \dots, \mu_n$  and relevant thicknesses  $t_1, t_2, \dots, t_n$  between the source and the detector active medium. All the attenuations are calculated as the total attenuation coefficient without coherent scattering even for the detector medium attenuation. The attenuation factor,  $f_{att}$ , is given by

$$f_{att} = e^{-\sum_{i=1}^n \mu_i t_i} \tag{5}$$

where

$\delta_i = \left( \frac{t_i}{\cos \theta} \right)$  for a Plexiglas horizontal layer, which is used to support the sources,

and for support and housing layers is calculated as

$$\delta_i = \sqrt{(R_d + t_i)^2 - [\rho^2 + (h + R_d)^2] \sin^2 \theta} - \sqrt{(R_d + t_{i-1})^2 - [\rho^2 + (h + R_d)^2] \sin^2 \theta}, \tag{6}$$

where  $t_i = \sum_{j=1}^i x_j$  and  $i$  starts from the detector and increases towards the outer surface.

This case can be extended to calculate the effective solid angle  $\Omega_{Cyl[Axial]}$  of a spherical detector subtended by a radioactive cylindrical source of radius,  $R_s$ , and height,  $h_s$ , as shown in Fig. 2, and is given by

$$\Omega_{Cyl[Axial]} = \frac{1}{\pi R_s^2 h_s} \int_{h_0}^{h_0+h_s} \int_0^{2\pi} \int_0^{R_s} \int_0^{\theta'_{max}} \int_0^{2\pi} S_f f_{att} (1 - e^{-\mu d}) \rho \sin \theta \, d\varphi d\theta d\rho dz \tag{7}$$

Based on the radioactive cylindrical source and NaI(Tl) spherical detector arrangement, the maximum polar angle in this case,  $\theta'_{max}$ , can be represented as

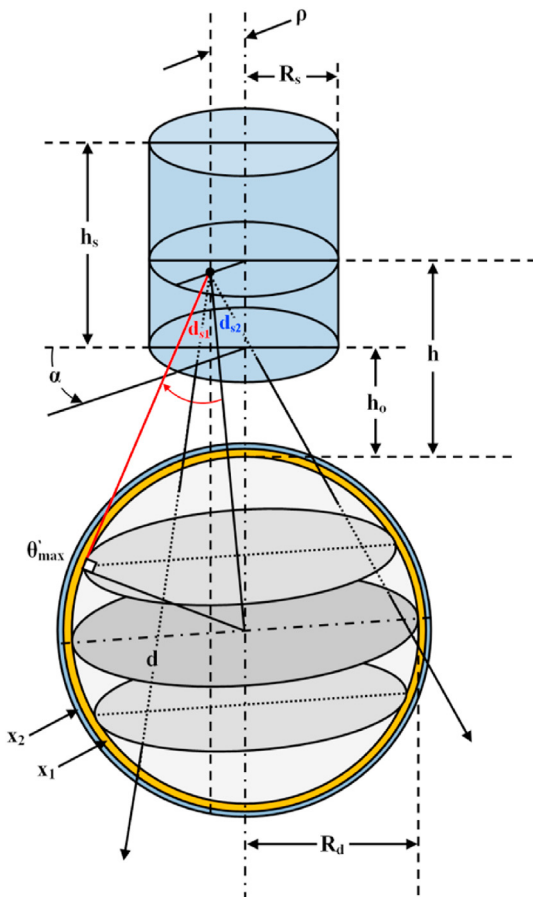


Fig. 2. Radioactive cylindrical source placed at a distance,  $h_0$ , from the NaI(Tl) spherical detector active medium surface.

$$\theta'_{max} = \sin^{-1} \left( \frac{R_d}{\sqrt{\rho^2 + (R_d+h)^2}} \right) \tag{8}$$

where  $\rho$  ranges from 0 to  $R_s$ , which is the radius of the radioactive cylinder.

The source self-absorption factor,  $S_f$  [22], can be calculated as a function of the attenuation of the radioactive source matrix,  $\mu_s$

$$S_f = e^{-\mu_s d_s} \tag{9}$$

By use of Fig. 3, the distance traveled by the photons through the source material,  $d_s$ , can be calculated by formulas

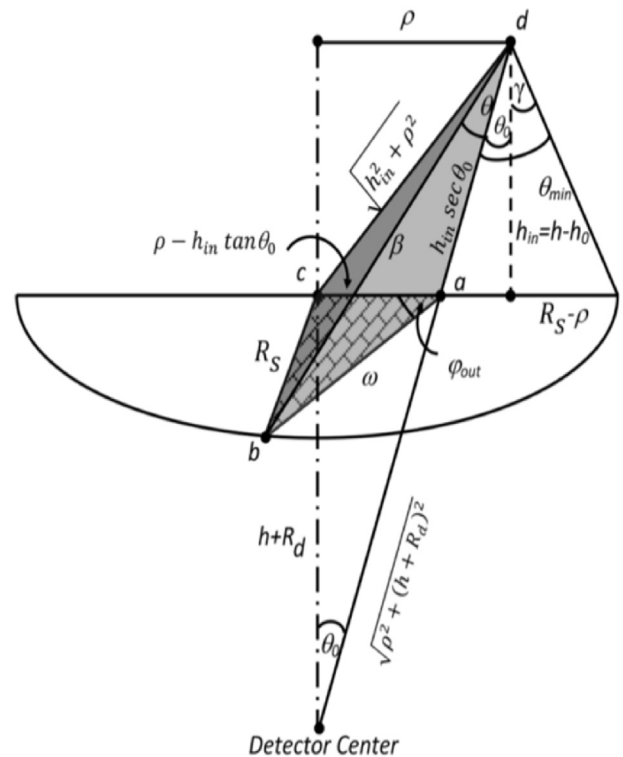


Fig. 3. Cross-sectional drawing of the radioactive cylindrical source to NaI(Tl) spherical detector center.

$$d_s = \begin{cases} \frac{\rho \cos \varphi + \sqrt{R_s - \rho^2 \sin^2 \theta}}{\sin \theta} & \text{if } R_s < R_d \\ \frac{h_{in}}{\cos \theta} & \text{otherwise,} \end{cases} \quad (10)$$

where  $\theta_{min}$  and  $\varphi_{out}$  are the polar and azimuthal angles, which determine the photon path-length through the source material and can be expressed as

$$\theta_{min} = \theta_0 + \gamma = \cos^{-1} \left( \frac{h_{in}(R_d + h) - \rho(R_s - \rho)}{\sqrt{h_{in}^2 + (R_s - \rho)^2} \sqrt{\rho^2 + (h + R_d)^2}} \right) \quad (11)$$

$$\varphi_{out} = \cos^{-1} \left( \frac{(\rho - h_{in} \tan \theta_0)^2 + \omega^2 - R_s^2}{2(\rho - h_{in} \tan \theta_0)\omega} \right) \quad (12)$$

where in the triangle  $dab$ , as shown in Fig. 3,

$$\frac{\omega}{\sin \theta} = \frac{h_{in} \sec \theta_0}{\cos \theta} \quad (13)$$

$$\omega = h_{in} \sec \theta_0 \tan \theta. \quad (14)$$

By substituting Eq. (14) in Eq. (12), one can find that

$$\varphi_{out} = \cos^{-1} \left( \frac{(\rho - h_{in} \tan \theta_0)^2 + (h_{in} \sec \theta_0 \tan \theta)^2 - R_s^2}{2(\rho - h_{in} \tan \theta_0)(h_{in} \sec \theta_0 \tan \theta)} \right) \quad (15)$$

$$\tan \theta_0 = \frac{\rho}{h + R_d} \quad (16)$$

$$\sec \theta_0 = \frac{\sqrt{\rho^2 + (h + R_d)^2}}{h + R_d} \quad (17)$$

In this case, the attenuation factor  $f_{att}$  for all absorbers between the source and the detector active medium can be calculated from Eqs. (5) and (6), and the attenuation of the cylindrical vial of the radioactive source is added to  $f_{att}$  under the following conditions for the parameter  $\delta_i$

$$\delta_i = \begin{cases} \left( \frac{t_i}{\sin \theta} \right) & \text{if } R_s < R_d \text{ and } \theta_{min} < \theta < \theta_{max} \text{ and } \varphi \geq \varphi_{out}, \\ \left( \frac{t_i}{\cos \theta} \right) & \text{otherwise.} \end{cases} \quad (18)$$

The full-energy peak efficiency for a radioactive axial point source and a spherical NaI(Tl) detector can be calculated through the NSM, based on the efficiency transfer method, and is given by

$$\varepsilon_{P(Point)} = \frac{\Omega_{Point[Axial]}}{\Omega_{ref[Axial]}} \varepsilon_{ref[Axial]} \quad (19)$$

where  $\varepsilon_{P(Point)}$  and  $\varepsilon_{ref[Axial]}$  are the full-energy peak efficiency of the spherical NaI(Tl) detector for the point-source reference and sought the point-source position, where the source in both cases is located axially at a certain (possibly different) distance from the front surface of the spherical NaI(Tl) detector, respectively. The measurement at the reference position must be taken without the CS

phenomenon. Therefore, the radioactive axial point source is placed at a sufficient distance from the detector active medium surface to avoid these effects.

$\Omega_{Point[Axial]}$  and  $\Omega_{ref[Axial]}$  are the effective solid angles subtended by the spherical NaI(Tl) detector surface and the axial point source and can be calculated from Eq. (2), where the source is in an axial position and the new efficiency calculation can be done for an axial position at different distances from the reference position. By the same concept, the full-energy peak efficiency for a radioactive cylindrical source with the spherical NaI(Tl) detector can be calculated by the following equation

$$\varepsilon_{P(Cyl)} = \frac{\Omega_{Cyl[Axial]}}{\Omega_{ref[Axial]}} \varepsilon_{ref[Axial]} \quad (20)$$

where  $\varepsilon_{P(Cyl)}$  is the full-energy peak efficiency of the spherical NaI(Tl) detector for the cylindrical-source geometry, where the source is located axially at a certain distance from the front surface of the spherical NaI(Tl) detector.  $\Omega_{Cyl[Axial]}$  is the effective solid angle subtended by the spherical NaI(Tl) detector surface concerning the axial radioactive cylindrical source and can be calculated by Eq. (7), where the radioactive cylindrical source is located at an axial position different from the reference position. The total efficiency,  $\varepsilon_{T(Cyl)}$ , of the spherical NaI(Tl) detector with a radioactive cylindrical source is given by the following equation

$$\varepsilon_{T(Cyl)} = \frac{\Omega_{Cyl[Axial]}}{4\pi} \quad (21)$$

The numerical trapezoidal rule has been used to calculate the effective solid angle of the spherical NaI(Tl) detector in both cases: axial radioactive point source and cylindrical source. A computer program has been used to increase the precision of the double integration by increasing the number of intervals in the integration. The calculations of the corrections of the  $\gamma$ - $\gamma$  CS factors are performed for each peak in the  $^{152}\text{Eu}$  radioactive cylindrical source gamma spectrum, employing the nuclear data from the decay scheme and Eqs. (20) and (21) as well, according to the summing-in (increase in the number of counts of the spectrum) or summing-out (decrease in the number of counts in the spectrum) effect. The  $\gamma$ - $\gamma$  CS factors,  $(CS)_{\gamma_{ij}}$ , can be obtained as in Refs. [23,24] by the following equation for each energy of the gamma-ray emitted in the transition from the state  $I$  to state  $J$

$$(CS)_{\gamma_{ij}} = ABC \quad (22)$$

where  $A$  represents the coincidences with gamma-ray lines preceding the  $\gamma_{ij}$  line,  $B$  represents the coincidences with gamma-ray lines following the  $\gamma_{ij}$  line, and  $C$  represents coincidences of gamma-ray lines, where the sum of the energies is equal to  $E_{ij}$ .

### 3. Experimental equipment, data collection, and analysis

The spherical NaI(Tl) scintillation detector is from SCIONIX (Netherlands): model number C76B80/2M-Q-X with the following geometrical dimensions: a crystal with a diameter of 76 mm, a reflector made of polytetrafluoroethylene with a thickness of 2 mm, and an aluminum cover with a thickness of 1 mm, resulting in maximum outer diameter of the detector of 83 mm (including the rim of the cover) and a volume of approximately 230 cm<sup>3</sup>. More details are shown in Fig. 4. The detector is optically coupled to a photomultiplier tube of the head-on type by Hamamatsu (model R6231, serial number S23185) with a diameter of 51 mm, a bi-alkali photocathode (with an effective circular area with a diameter of 46 mm and a spectral response covering the wavelength range

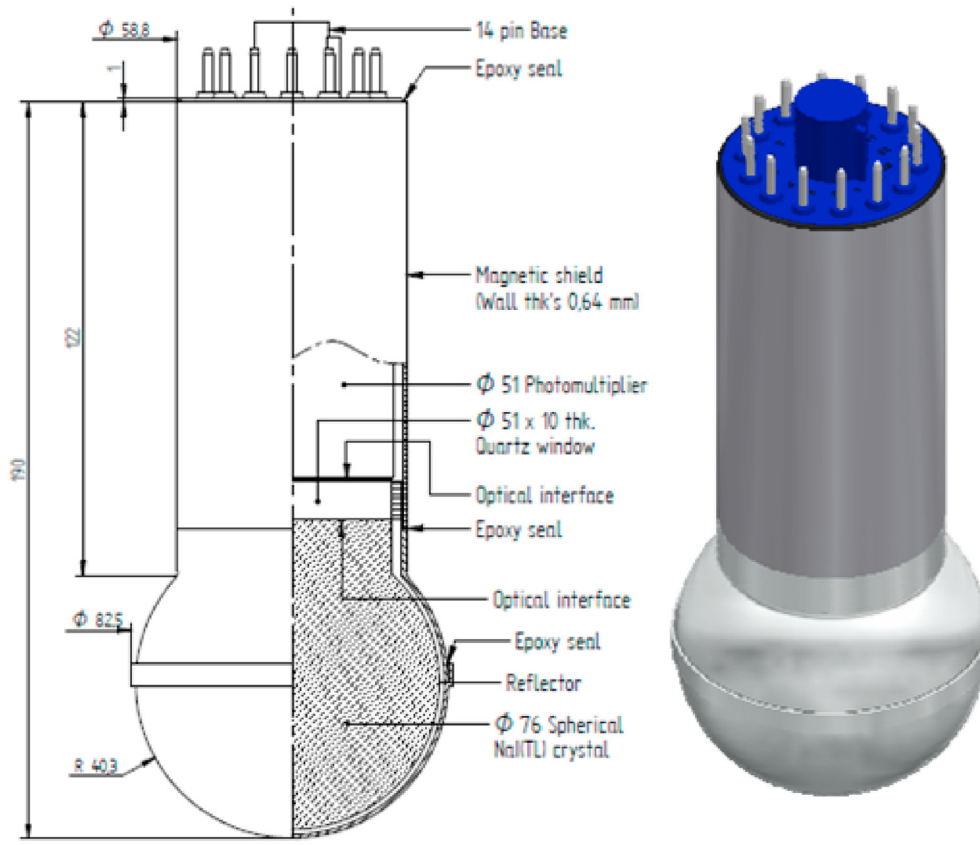


Fig. 4. Manufacturer details of the spherical NaI(Tl) detector.

300–650 nm), and a 14-pin base. It was developed specifically for the detection of gamma-rays over a wide energy range. The average energy resolution for the 662 keV gamma-rays of  $^{137}\text{Cs}$  is 8.6% (Full Width at Half Maximum, FWHM). The detector has high efficiency

because the crystal has a large enough cross-section for gamma-ray interactions and the operating voltage of 770 V is enough to achieve saturation.

The pulses from the spherical NaI(Tl) detector have been recorded in digital form and stored on the hard disk of a personal computer for extra offline analysis. The spectra have been recorded and processed with the winTMCA32 and analyzed with the Genie 2000 data acquisition and analysis software package [Ver. 3.2.3 (S501)]. It contains a spectral display, basic spectrum analysis, and recording. The acquisition and storing system consists of 1000-channel data acquisition (“MCA Control”) and a software package that includes a management program and an event-building program. It also has tools to support multiple analysis algorithms for a given analysis step via the interactive graphical user interface, such as background subtraction, reference peak correction, and interactive peak fit.

Five radioactive point sources ( $^{241}\text{Am}$ ,  $^{133}\text{Ba}$ ,  $^{137}\text{Cs}$ ,  $^{60}\text{Co}$ , and  $^{152}\text{Eu}$ ) were purchased from the Physikalisch-Technische Bundesanstalt (PTB, Germany); they emit photons with energies from 59.53 keV to 1408.01 keV. The activity of these sources was  $259.0 \pm 2.6$  kBq,  $275.3 \pm 2.8$  kBq,  $285.0 \pm 4.0$  kBq,  $212.1 \pm 1.5$  kBq, and  $290.0 \pm 4.0$  kBq, respectively, on June 1, 2009. These sources have been measured separately at a distance from the detector surface of 22.28 cm, 30.02 cm, 37.76 cm, 45.50 cm, and 53.24 cm, respectively, with tolerances  $\pm 0.2$  cm. The measurement at 53.24 cm (which can be considered a large distance when compared to the diameter of the detector) is used to obtain the efficiency curve, which is free from the CS phenomenon. At this position, the dead time is almost zero. The curve obtained under this condition is suitable as a reference curve. Therefore, it can be used to calculate the efficiency curve at any other location



Fig. 5. Plexiglas holder and radioactive source measurements.



employing Eq. (19).

The cylindrical radioactive source is made from  $^{152}\text{Eu}$  dispersed in a water matrix kept in a polypropylene vial with bottom and side thicknesses of 0.11 cm. The source has a radius  $R_s = 1.87$  cm and height  $h_s = 4.54$  cm. The activity was  $5048 \pm 99$  Bq on January 1, 2010 at 00:00 CET. This source emits gamma-rays with energies from 121.78 keV to 1408.01 keV. It has been placed at a distance of 0.724 cm from the detector end cap. The effect of the  $\gamma$ - $\gamma$  CS phenomenon on the detector efficiency has been studied with this radioactive cylindrical source, where the full-energy peak efficiency is calculated by Eq. (20) with 53.24 cm as the reference distance. The Plexiglas holder has been used during all these measurements to achieve high accuracy in the positioning, while the detector housing, which carries the holder, is made of Teflon, as shown in Fig. 5.

The efficiency calibration of a spherical NaI(Tl) detector with standard radioactive point sources should be performed at regular times every year. The measured full-energy peak efficiency,  $\varepsilon_P(E)$ , for the spherical NaI(Tl) detector is obtained from the following equation for each gamma-ray emitted by the radionuclide sources used

$$\varepsilon_P(E) = \frac{N(E)}{TAI(E)} \quad (23)$$

where  $N(E)$  is the net peak area obtained for every full-energy peak corresponding to an energy  $E$  with a suitable fit function for the NaI(Tl) detector,  $T$  is the live time of the acquisition,  $A$  is the activity of the radioisotope source at the time of measurement, and  $P(E)$  is the probability of gamma disintegration of the radionuclide leading to the emission of a gamma-ray with energy  $E$ .

The uncertainty,  $\sigma_\varepsilon$ , of the measured full-energy peak efficiency,  $\varepsilon_P(E)$ , is given by

$$\sigma_\varepsilon = \sqrt{\left(\frac{\partial \varepsilon}{\partial A}\right)^2 \sigma_A^2 + \left(\frac{\partial \varepsilon}{\partial P}\right)^2 \sigma_P^2 + \left(\frac{\partial \varepsilon}{\partial N}\right)^2 \sigma_N^2} \quad (24)$$

where  $\sigma_A$ ,  $\sigma_P$  and  $\sigma_N$  are the uncertainties associated with the quantities  $A$ ,  $P(E)$ , and  $N(E)$ , respectively.

In the case of the  $^{152}\text{Eu}$  radioactive cylindrical source, which has been positioned very close to the detector, thus affected by the  $\gamma$ - $\gamma$  CS phenomenon, the measured full-energy peak efficiency,  $\varepsilon'_P(E)$ , is given as

$$\varepsilon'_P(E) = \frac{N'(E)}{TAP(E)} \quad (25)$$

where  $N'(E)$  is the net area under the full-energy peak with the CS phenomenon.

The general form of the  $\gamma$ - $\gamma$  (CS) $_{\gamma_{ij}}$  factor for each gamma-ray energy line,  $\gamma_{ij}$ , is defined as

$$(CS)_{\gamma_{ij}} = \frac{N(E)}{N'(E)} \quad (26)$$

where  $N(E)$  is the net area under the full-energy peak without the CS phenomenon.

To obtain the full-energy peak efficiency,  $\varepsilon_P(E)$ , for the  $^{152}\text{Eu}$  radioactive cylindrical source, such as in Eq. (23), Eqs. (25) and (26) must be multiplied together as shown in the following equation

$$\varepsilon_P(E) = \varepsilon'_P(E)(CS)_{\gamma_{ij}} \quad (27)$$

#### 4. Results and discussion

The energy calibration of the spherical NaI(Tl) detector is used to determine the relationship between the energy of the gamma-ray sources and the number of amplitude channels in the multi-channel analyzer. This procedure has been carried out by the winTMCA32 software, which is used as a multichannel analyzer with a tube base for scintillation spectrometry, after choosing an energy range based on the available standard radioactive sources. All the measured efficiency curves have been obtained with the probability of occurrence of every transition.

The energy resolution of the spherical NaI(Tl) detector is approximately 8.8% (FWHM) for the 662 keV gamma rays from  $^{137}\text{Cs}$  in a configuration where the radioactive source can be considered as point-like. This result is close to the value stated by the manufacturer. The linear energy calibration, expressing the channel number,  $Ch(E)$ , as a function of the energy,  $E_\gamma$  is

$$Ch(E_\gamma) = A + BE_\gamma \quad (28)$$

where  $E_\gamma$  is the gamma-ray energy in keV,  $Ch(E_\gamma)$  is the channel number in the spectra of the centroid of the peak matching the energy  $E_\gamma$ , and the calibration constants are  $A$  and  $B$ . The FWHM of the measured peaks as a function of the gamma-ray energy  $E_\gamma$ , has been fitted with a linear relation as

$$FWHM(E_\gamma) = C + D.E_\gamma \quad (29)$$

where  $C$  and  $D$  are constants. The measured values of the efficiency as a function of position are fitted with a polynomial function of fifth-order

$$\varepsilon_P(E_\gamma) = a_0 + a_1 E_\gamma + a_2 E_\gamma^2 + a_3 E_\gamma^3 + a_4 E_\gamma^4 \quad (30)$$

where  $a_0$ ,  $a_1$ ,  $a_2$ ,  $a_3$ , and  $a_4$  are constants.

The results obtained with the standard ( $^{137}\text{Cs}$  and  $^{60}\text{Co}$ ) radioactive point sources, positioned for the calibration at a distance of 22.28 cm, are shown in Figs. 6 and 7.

The measured full-energy peak efficiency curves,  $\varepsilon_P(E)$ , at different heights above the detector surface (22.28 cm, 30.02 cm, 37.76 cm, 45.50 cm, and 53.24 cm) with the associated uncertainty as a function of the photon energy are given in Fig. 8. At all these locations, the  $\gamma$ - $\gamma$  CS phenomenon is ignored because of the large distance between the source and the detector system. The measured detector efficiency decreases with the increase of source-to-detector distance according to the inverse square law.

Table 1 shows the reference values of  $Q_{\text{ref}[Axial]}$  and  $\varepsilon_P(E)$  with their uncertainties as a function of the photon energy (keV) at the reference location, and the effective solid angle ratios for the spherical NaI(Tl) detector. The ratio increases with decreasing source-to-detector distance. Table 2 gives a comparison between the measured  $\varepsilon_P(E)$ , with their uncertainties, as a function of the photon energy at the different locations and the efficiencies calculated by the NSM, based on Eq. (19), for the spherical NaI(Tl) detector with radioactive point sources. In general, the discrepancies  $\Delta\%$  are less than 6% between the measured efficiency,  $\varepsilon_P(E)$ , and the efficiency calculated by the NSM. They are obtained as

$$\Delta\% = \frac{\varepsilon_{\text{Calculated (NSM)}} - \varepsilon_P(E)}{\varepsilon_{\text{Calculated (NSM)}}} \times 100, \quad (31)$$

where  $\varepsilon_{\text{Calculated(NSM)}}$  is the full-energy peak efficiency calculated with the NSM.

The measured reference efficiency curve is obtained by using radioactive point sources at 53.24 cm. The effective solid angle is

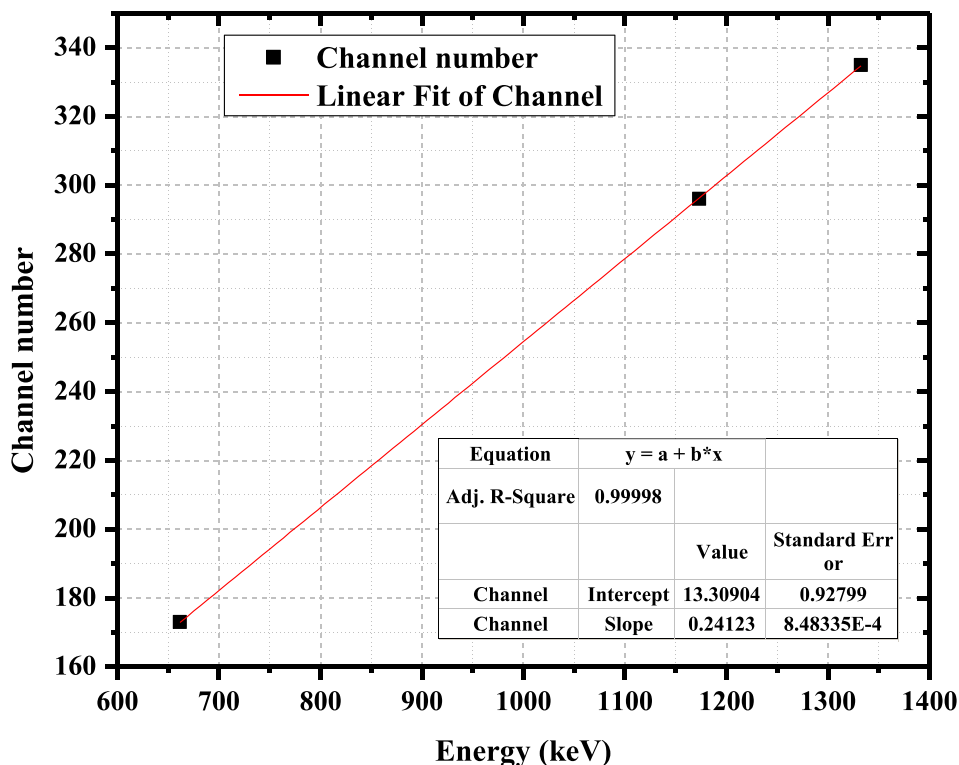


Fig. 6. The measured and the fit calibration energy curve for using standard (137Cs and 60Co) radioactive point sources with spherical NaI(Tl) detector.

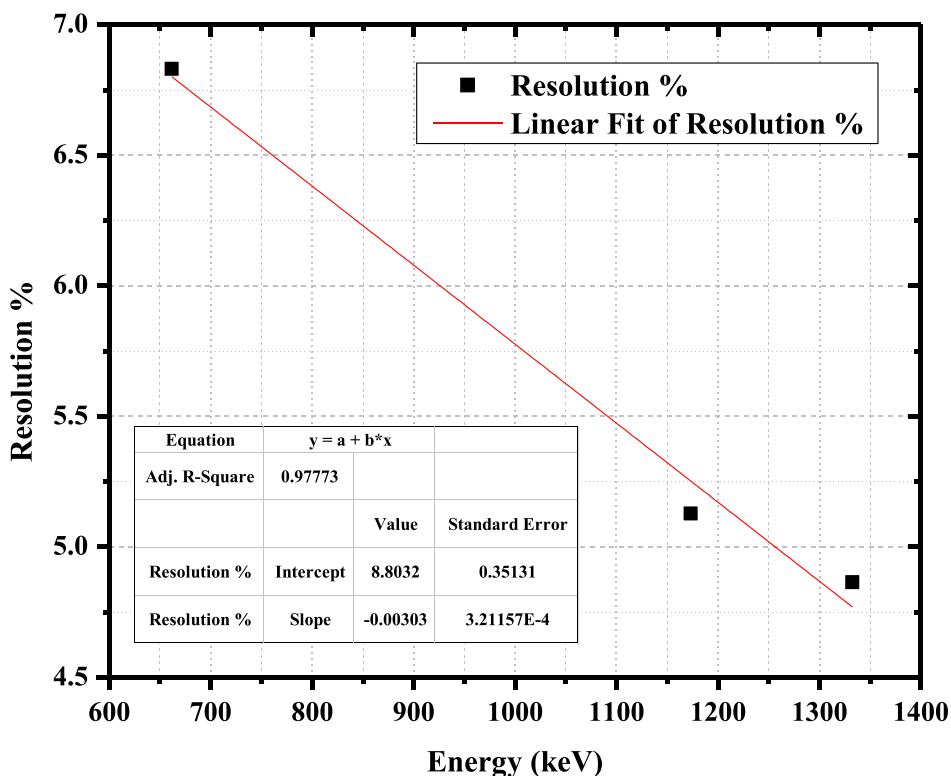


Fig. 7. The measured and the fit calibration shape curve for using standard (137Cs and 60Co) radioactive point sources with spherical NaI(Tl) detector.

used to obtain the full-energy peak efficiency for a radioactive cylindrical source by the NSM based on Eq. (20), while the total efficiency is obtained from Eq. (21). The full-energy peak efficiency

and the total efficiency are used to calculate the  $\gamma$ - $\gamma$  (CS) $_{\gamma\gamma}$  factors based on Eq. (22). The corrected measured efficiency in the case of the radioactive cylindrical source can be obtained from Eq. (27).

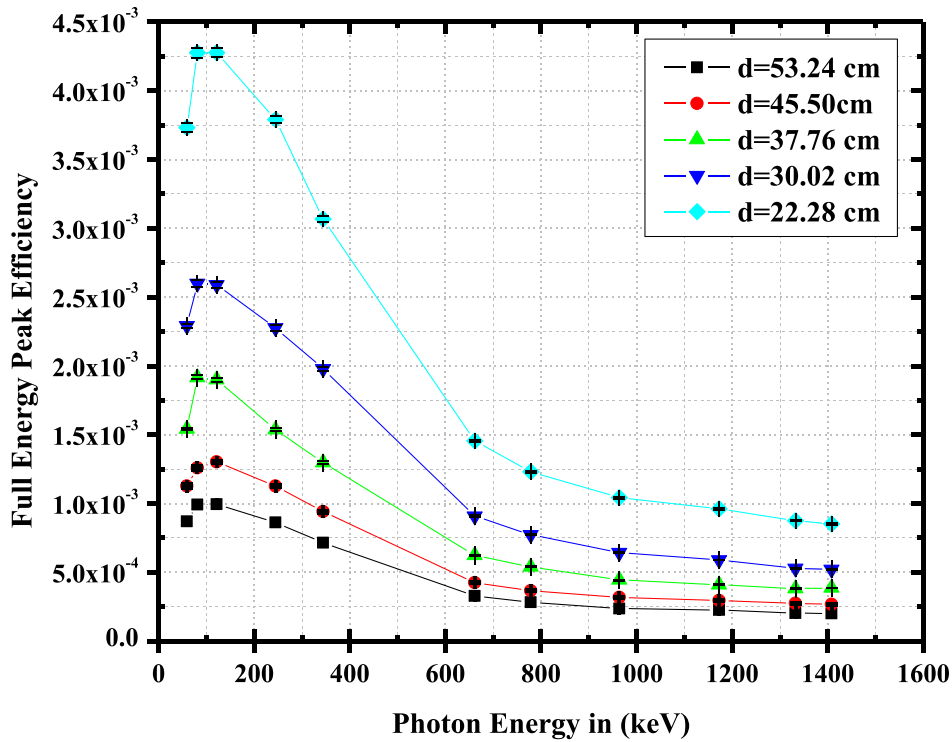


Fig. 8. The measured full-energy peak efficiency values of the spherical NaI(Tl) detector with their uncertainties as a function of the photon energy (keV) at different locations.

Table 1

The reference values [  $\Omega_{ref[Axial]}$  and  $\epsilon_P(E)$  ] and the effective solid angles ratios for a spherical NaI(Tl) detector.

Reference Values at 53.24 cm					Effective Solid Angle Ratios			
Nuclide	Energy (keV)	$\Omega_{ref[Axial]}$	Measured $\epsilon_P(E_\gamma)$	$\sigma_{\epsilon_P(E_\gamma)}$	$\frac{\Omega_{Point[45.5cm]}}{\Omega_{ref[53.24cm]}}$	$\frac{\Omega_{Point[37.76cm]}}{\Omega_{ref[53.24cm]}}$	$\frac{\Omega_{Point[30.02cm]}}{\Omega_{ref[53.24cm]}}$	$\frac{\Omega_{Point[22.28cm]}}{\Omega_{ref[53.24cm]}}$
<sup>241</sup> Am	59.53	1.140E-02	8.701E-04	8.328E-06	1.342	1.880	2.832	4.746
<sup>133</sup> Ba	80.99	1.176E-02	9.930E-04	5.964E-06	1.337	1.878	2.829	4.741
<sup>152</sup> Eu	121.78	1.198E-02	9.943E-04	8.049E-06	1.336	1.876	2.823	4.720
<sup>152</sup> Eu	244.69	1.165E-02	8.619E-04	6.684E-06	1.336	1.877	2.828	4.740
<sup>152</sup> Eu	344.28	1.083E-02	7.159E-04	5.464E-06	1.337	1.879	2.830	4.737
<sup>137</sup> Cs	661.66	9.140E-03	3.283E-04	2.034E-06	1.337	1.877	2.828	4.740
<sup>152</sup> Eu	778.91	8.760E-03	2.829E-04	2.272E-06	1.337	1.877	2.828	4.740
<sup>152</sup> Eu	964.13	8.280E-03	2.359E-04	1.906E-06	1.336	1.877	2.827	4.739
<sup>60</sup> Co	1173.23	7.820E-03	2.255E-04	1.032E-06	1.336	1.877	2.827	4.731
<sup>60</sup> Co	1332.50	7.550E-03	2.031E-04	9.286E-07	1.338	1.875	2.821	4.742
<sup>152</sup> Eu	1408.01	7.440E-03	2.013E-04	1.474E-06	1.337	1.883	2.796	4.691

Table 3 gives a comparison between the measured  $\epsilon_P(E)$  with its uncertainty, the measured full-energy peak efficiency, before and after the correction for  $\gamma$ - $\gamma$  CS phenomenon is applied, and the full-energy peak efficiency calculated by the NSM for the spherical NaI(Tl) detector with a radioactive cylindrical source located at 0.724 cm. The discrepancy,  $\Delta_1\%$ , between the measured full-energy peak efficiency  $\epsilon_P(E_\gamma)$  and the full-energy peak efficiency calculated by the NSM  $\epsilon_{Calculated (NSM)}(E_\gamma)$  is quantified by

$$\Delta_1\% = \frac{\epsilon_{Calculated (NSM)}(E_\gamma) - \epsilon_P(E_\gamma)}{\epsilon_{Calculated (NSM)}(E_\gamma)} \times 100 \quad (32)$$

The discrepancy,  $\Delta_2\%$ , between the corrected measured full-energy peak efficiency  $\epsilon_{P(Corrected)}(E_\gamma)$  and the full-energy peak efficiency calculated by the NSM  $\epsilon_{Calculated (NSM)}(E_\gamma)$  is given by

$$\Delta_2\% = \frac{\epsilon_{Calculated (NSM)}(E_\gamma) - \epsilon_{P(Corrected)}(E_\gamma)}{\epsilon_{Calculated (NSM)}(E_\gamma)} \times 100 \quad (33)$$

The results show that the effects of the corrections for  $\gamma$ - $\gamma$  CS phenomenon increase the measured efficiencies, which have been measured with the source positioned close to the detector surface. The discrepancy  $\Delta_2\%$  between the corrected measured full-energy peak efficiency and the full-energy peak efficiency calculated by the NSM is less than 1%. The discrepancy  $\Delta_1\%$  between the measured full-energy peak efficiency and the full-energy peak efficiency calculated by the NSM is almost 11%. Thus, the method presented provides a quick and straightforward way for the determination of the detector efficiency.

The positions of the radioactive sources have been estimated to have a tolerance of  $\pm 0.2$  cm, which has been propagated to the solid angle considering the difference between the reference and the



**Table 2**  
Comparison between the measured efficiencies,  $\epsilon_P(E)$ , with their uncertainties, and the calculated efficiencies by (NSM) for the spherical NaI(Tl) detector using radioactive point sources at different locations.

Distance 45.50 cm						Distance 37.76 cm			
Nuclide	Energy (keV)	Measured $\epsilon_P(E_\gamma)$	$\sigma_{\epsilon_P(E_\gamma)}$	NSM	$\Delta\%$	Measured $\epsilon_P(E_\gamma)$	$\sigma_{\epsilon_P(E_\gamma)}$	NSM	$\Delta\%$
<sup>241</sup> Am	59.53	1.128E-03	1.555E-05	1.168E-03	3.43	1.556E-03	9.895E-06	1.636E-03	4.87
<sup>133</sup> Ba	80.99	1.259E-03	1.202E-05	1.327E-03	5.14	1.916E-03	1.356E-05	1.864E-03	-2.75
<sup>152</sup> Eu	121.78	1.302E-03	1.050E-05	1.329E-03	2.00	1.900E-03	1.529E-05	1.865E-03	-1.90
<sup>152</sup> Eu	244.69	1.127E-03	8.841E-06	1.152E-03	2.14	1.537E-03	1.205E-05	1.618E-03	5.03
<sup>152</sup> Eu	344.28	9.413E-04	7.201E-06	9.572E-04	1.66	1.297E-03	9.898E-06	1.345E-03	3.59
<sup>137</sup> Cs	661.66	4.240E-04	2.540E-06	4.390E-04	3.40	6.220E-04	3.332E-06	6.164E-04	-0.91
<sup>152</sup> Eu	778.91	3.668E-04	2.981E-06	3.782E-04	3.01	5.400E-04	4.335E-06	5.310E-04	-1.70
<sup>152</sup> Eu	964.13	3.168E-04	2.588E-06	3.151E-04	-0.52	4.440E-04	3.586E-06	4.428E-04	-0.27
<sup>60</sup> Co	1173.23	2.954E-04	1.187E-06	3.013E-04	1.94	4.096E-04	1.753E-06	4.233E-04	3.22
<sup>60</sup> Co	1332.50	2.740E-04	1.100E-06	2.716E-04	-0.87	3.827E-04	1.636E-06	3.808E-04	-0.50
<sup>152</sup> Eu	1408.01	<b>2.664E-04</b>	<b>1.959E-06</b>	<b>2.692E-04</b>	<b>1.05</b>	<b>3.865E-04</b>	<b>2.842E-06</b>	<b>3.791E-04</b>	<b>-1.97</b>

Distance 30.02 cm						Distance 22.28 cm			
Nuclide	Energy (keV)	Measured $\epsilon_P(E_\gamma)$	$\sigma_{\epsilon_P(E_\gamma)}$	NSM	$\Delta\%$	Measured $\epsilon_P(E_\gamma)$	$\sigma_{\epsilon_P(E_\gamma)}$	NSM	$\Delta\%$
<sup>241</sup> Am	59.53	2.342E-03	1.489E-05	2.464E-03	4.93	3.932E-03	3.253E-05	4.129E-03	-5.02
<sup>133</sup> Ba	80.99	2.700E-03	2.733E-05	2.809E-03	3.90	4.475E-03	3.364E-05	4.708E-03	-5.21
<sup>152</sup> Eu	121.78	2.690E-03	2.101E-05	2.807E-03	4.18	4.477E-03	3.414E-05	4.694E-03	-4.85
<sup>152</sup> Eu	244.69	2.376E-03	1.862E-05	2.438E-03	2.51	3.990E-03	2.687E-05	4.085E-03	-2.39
<sup>152</sup> Eu	344.28	2.078E-03	1.517E-05	2.026E-03	-2.55	3.269E-03	2.432E-05	3.391E-03	-3.73
<sup>137</sup> Cs	661.66	9.086E-04	4.980E-06	9.286E-04	2.15	1.604E-03	9.328E-06	1.556E-03	2.98
<sup>152</sup> Eu	778.91	7.735E-04	6.491E-06	8.000E-04	3.31	1.350E-03	8.802E-06	1.341E-03	0.66
<sup>152</sup> Eu	964.13	6.447E-04	5.463E-06	6.670E-04	3.35	1.143E-03	7.595E-06	1.118E-03	2.20
<sup>60</sup> Co	1173.23	6.391E-04	2.624E-06	6.375E-04	-0.26	1.017E-03	4.166E-06	1.067E-03	-4.89
<sup>60</sup> Co	1332.50	5.494E-04	2.355E-06	5.729E-04	4.09	9.746E-04	3.738E-06	9.628E-04	1.21
<sup>152</sup> Eu	1408.01	5.398E-04	3.966E-06	5.628E-04	4.09	9.532E-04	6.032E-06	9.443E-04	0.93

**Table 3**  
Comparison between the measured efficiency, the  $(CS)_{\gamma,II}$  factors, the corrected efficiencies by (NSM) and the discrepancies at 0.724 cm from the surface of the spherical NaI(Tl) detector.

Nuclide	Energy (keV)	Measured $\epsilon_P(E_\gamma)$	$\sigma_{\epsilon_P(E_\gamma)}$	NSM	$\Delta_1\%$	$(CS)_{\gamma,II}$	Corrected Measured $\epsilon_P(E_\gamma)$	$\Delta_2\%$
<sup>152</sup> Eu	121.78	4.026E-02	6.691E-06	4.441E-02	9.35	1.1067	4.455E-02	-0.32
<sup>152</sup> Eu	244.69	3.704E-02	7.789E-06	4.112E-02	11.00	1.1168	4.137E-02	-0.61
<sup>152</sup> Eu	344.28	3.304E-02	5.623E-06	3.530E-02	6.85	1.0757	3.554E-02	-0.67
<sup>152</sup> Eu	778.91	1.402E-02	3.188E-06	1.506E-02	7.44	1.0828	1.518E-02	-0.78
<sup>152</sup> Eu	964.13	1.190E-02	2.510E-06	1.280E-02	7.57	1.0799	1.285E-02	-0.39
<sup>152</sup> Eu	1408.01	1.061E-02	1.844E-06	1.129E-02	6.42	1.0621	1.127E-02	0.20

actual geometry as in Ref. [25]. The uncertainties evaluated in such a way are reported in Tables 2 and 3.

**5. Conclusions**

The present work provides a quick and straightforward method to calibrate a spherical NaI(Tl) gamma-ray detector by the NSM and to obtain its full-energy peak efficiency at different locations from the detector surface for radioactive point and cylindrical sources. The method has been used to correct the measured full-energy peak efficiency for the CS phenomenon with radioactive cylindrical sources positioned at a very short source-to-detector distance. A program has been written to solve the system of equations for the effective solid angle, full-energy peak efficiency, and total efficiency. Laboratory measurements have been made to study the validity of the CS approach and show a good match with the results obtained by the NSM. Within 6% mean confidence, the NSM can be used in the calibration process for gamma-ray detectors in the absence of standard radioactive calibration sources. The method is based on the effective solid angle ratio concept, considering the gamma-ray attenuation in the detector itself, the end cap, and the rest of the materials between the radioactive gamma-ray source and the detector. This work can be extended to calculate the full-energy peak efficiency for a spherical NaI(Tl) gamma-ray detector

with any other source geometry different from the radioactive cylindrical source.

**Author contributions**

Mohamed S. Badawi and Salam F. Nouredine developed the mathematical model and performed numerical testing. Mohamed S. Badawi and Salam F. Nouredine conceived and wrote the article. Mohamed S. Badawi and Mahmoud I. Abbas made valuable contributions in the experimental work. All authors extensively interacted with each other, exchanging ideas, especially during preparation of the manuscript.

**Declaration of competing interest**

The authors declare that they have no known competing financial interests or personal relationships that could have appeared to influence the work reported in this paper.

**Acknowledgments**

This work has been done in the frame of a scientific collaboration between the Physics Department, Faculty of Science, Alexandria University, Alexandria, Egypt, and the Physics Department,

Faculty of Science, Lebanese University, Beirut, Lebanon. The authors highly appreciate the Lebanese University for financial support and are thankful to Dr. Ayman Hamzawy and Dr. Abouzeid A. Thabet for their fruitful discussions.

## References

- [1] L. Moens, J. De Donder, L. Xi-lei, F. De Corte, A. De Wispelaere, A. Simonits, et al., Calculation of the absolute peak efficiency of gamma-ray detectors for different counting geometries, *Nucl. Instrum. Methods Phys. Res.* 187 (1981) 451–472, [https://doi.org/10.1016/0029-554x\(81\)90374-8](https://doi.org/10.1016/0029-554x(81)90374-8).
- [2] H.-X. Shi, B.-X. Chen, T.-Z. Li, D. Yun, Precise Monte Carlo simulation of gamma-ray response functions for an NaI(Tl) detector, *Appl. Radiat. Isot.* 57 (2002) 517–524, [https://doi.org/10.1016/s0969-8043\(02\)00140-9](https://doi.org/10.1016/s0969-8043(02)00140-9).
- [3] Y. Mian, D. Jie, W. Shan, Y. Zhang, C. Ma, A nuclear density probe: isobaric yield ratio difference, *Nucl. Sci. Tech.* 26 (2015), S20503, <https://doi.org/10.13538/j.1001-8042/nst.26.S20503>.
- [4] M.M. Gouda, M.S. Badawi, A.M. El-Khatib, M.M. Mohamed, A.A. Thabet, M.I. Abbas, Calibration of well-type NaI(Tl) detector using a point sources measured out the detector well at different axial distances, *J. Instrum.* 10 (2015), <https://doi.org/10.1088/1748-0221/10/03/p03022>.
- [5] M.I. Abbas, S. Noureddine, Analytical expression to calculate total and full-energy peak efficiencies for cylindrical phoswich and lanthanum bromide scintillation detectors, *Radiat. Meas.* 46 (2011) 440–445, <https://doi.org/10.1016/j.radmeas.2011.01.017>.
- [6] J.C. Aguiar, An analytical calculation of the peak efficiency for cylindrical sources perpendicular to the detector axis in gamma-ray spectrometry, *Appl. Radiat. Isot.* 66 (2008) 1123–1127, <https://doi.org/10.1016/j.apradiso.2007.12.007>.
- [7] H.M. Al-Arbawy, Study the effect of the shields movement and its thickness in detection efficiency by using scintillation detector NaI(Tl), *Adv. Phys. Theor. Appl.* 31 (2014) 53–57.
- [8] A. Hamzawy, New analytical approach to calculate the detector efficiencies of NaI(Tl) using coaxial and off-axis rectangular and parallelepiped sources, *Nucl. Instrum. Methods Phys. Res. Sect. A Accel. Spectrom. Detect. Assoc. Equip.* 768 (2014) 164–169, <https://doi.org/10.1016/j.nima.2014.09.013>.
- [9] A. Hamzawy, D.N. Grozdanov, M.S. Badawi, F.A. Aliyev, A.A. Thabet, M.I. Abbas, et al., New numerical simulation method to calibrate the regular hexagonal NaI(Tl) detector with radioactive point sources situated non-axial, *Rev. Sci. Instrum.* 87 (2016) 115105, <https://doi.org/10.1063/1.4966990>.
- [10] M.-C. Lépy, T. Altizoglou, M.J. Anagnostakis, D. Arnold, M. Capogni, A. Ceccatelli, et al., Intercomparison of methods for coincidence summing corrections in gamma-ray spectrometry, *Appl. Radiat. Isot.* 68 (2010) 1407–1412, <https://doi.org/10.1016/j.apradiso.2010.01.012>.
- [11] D. Novković, M. Đurašević, A. Kandić, I. Vukanac, B. Šešlak, Z. Milošević, Coincidence summing corrections for point and volume <sup>152</sup>Eu sources, *Appl. Radiat. Isot.* 107 (2016) 138–144, <https://doi.org/10.1016/j.apradiso.2015.10.015>.
- [12] G. Giubrone, J. Ortiz, S. Gallardo, S. Martorell, M.C. Bas, Calculation of coincidence summing correction factors for an HPGe detector using GEANT4, *J. Environ. Radioact.* 158–159 (2016) 114–118, <https://doi.org/10.1016/j.jenvrad.2016.04.008>.
- [13] S.S. Nafee, M.S. Badawi, A.M. Abdel-Moneim, S.A. Mahmoud, Calibration of the 4 $\pi$   $\gamma$ -ray spectrometer using a new numerical simulation approach, *Appl. Radiat. Isot.* 68 (2010) 1746–1753, <https://doi.org/10.1016/j.apradiso.2010.02.013>.
- [14] A.M. El-Khatib, M.S. Badawi, M.A. Elzاهر, A.A. Thabet, A study of the validity of the efficiency transfer method to calculate the peak efficiency using  $\gamma$ -ray detectors at extremely large distances, *J. Theoret. Appl. Phys.* 8 (2014), <https://doi.org/10.1007/s40094-014-0120-1>.
- [15] M.I. Abbas, M.S. Badawi, I.N. Ruskov, A.M. El-Khatib, D.N. Grozdanov, A.A. Thabet, et al., Calibration of a single hexagonal NaI(Tl) detector using a new numerical method based on the efficiency transfer method, *Nucl. Instrum. Methods Phys. Res. Sect. A Accel. Spectrom. Detect. Assoc. Equip.* 771 (2015) 110–114, <https://doi.org/10.1016/j.nima.2014.10.056>.
- [16] M.M. Gouda, A. Hamzawy, M.S. Badawi, A.M. El-Khatib, A.A. Thabet, M.I. Abbas, Mathematical method to calculate full-energy peak efficiency of detectors based on transfer technique, *Indian J. Phys.* 90 (2015) 201–210, <https://doi.org/10.1007/s12648-015-0737-1>.
- [17] M.S. Badawi, I. Ruskov, M.M. Gouda, A.M. El-Khatib, M.F. Alotiby, M.M. Mohamed, et al., A numerical approach to calculate the full-energy peak efficiency of HPGe well-type detectors using the effective solid angle ratio, *J. Instrum.* 9 (2014), <https://doi.org/10.1088/1748-0221/9/07/p07030>.
- [18] D. Al Oraini, Calibration of the absolute efficiency of well-type NaI(Tl) scintillation detector in 0.121–1.408 MeV energy range, *Sci. Technol. Nuclear Install.* (2018) 1–6, <https://doi.org/10.1155/2018/6432380>.
- [19] C.-Y. Yi, S.-H. Hah, Monte Carlo calculation of response functions to gamma-ray point sources for a spherical NaI(Tl) detector, *Appl. Radiat. Isot.* 70 (2012) 2133–2136, <https://doi.org/10.1016/j.apradiso.2012.02.081>.
- [20] S. Byun, W. Prestwich, K. Chin, F. McNeill, D. Chettle, Efficiency calibration and coincidence summing correction for a 4 $\pi$  NaI(Tl) detector array, *Nucl. Instrum. Methods Phys. Res. Sect. A Accel. Spectrom. Detect. Assoc. Equip.* 535 (2004) 674–685, [https://doi.org/10.1016/s0168-9002\(04\)01469-x](https://doi.org/10.1016/s0168-9002(04)01469-x).
- [21] A. Thabet, A. Dlabac, S. Jovanovic, M. Badawi, N. Mihaljevic, A. El-Khatib, et al., Experimental verification of gamma-efficiency calculations for scintillation detectors in ANGLE 4 software, *Nucl. Technol. Radiat. Protect.* 30 (2015) 35–46, <https://doi.org/10.2298/ntrp1501035t>.
- [22] S. Noureddine, M. Badawi, M. Abbas, A hybrid analytical-numerical method for efficiency calculations of spherical scintillation NaI(Tl) detectors and arbitrarily located point sources, *Nucl. Technol. Radiat. Protect.* 32 (2017) 140–147, <https://doi.org/10.2298/ntrp1702140n>.
- [23] A. El-Khatib, A. Thabet, M. Elzاهر, M. Badawi, B. Salem, Study on the effect of the self-attenuation coefficient on  $\gamma$ -ray detector efficiency calculated at low and high energy regions, *Nuclear Eng. Technol.* 46 (2014) 217–224, <https://doi.org/10.5516/net.04.2013.077>.
- [24] A.M. El-Khatib, B.A. Salem, M.S. Badawi, M.M. Gouda, A.A. Thabet, M.I. Abbas, Full-Energy peak efficiency of an NaI(Tl) detector with coincidence summing correction showing the effect of the source-to-detector distance, *Chin. J. Phys.* 55 (2017) 478–489, <https://doi.org/10.1016/j.cjph.2016.11.013>.
- [25] M.S. Badawi, S.I. Jovanovic, A.A. Thabet, A.M. El-Khatib, A.D. Dlabac, B.A. Salem, et al., Calibration of 4 $\pi$  NaI(Tl) detectors with coincidence summing correction using new numerical procedure and ANGLE4 software, *AIP Adv.* 7 (2017), 035005, <https://doi.org/10.1063/1.4978214>.